

## BUCKLING OF IMPERFECT THICK CYLINDRICAL SHELLS AND CURVED PANELS WITH DIFFERENT BOUNDARY CONDITIONS UNDER EXTERNAL PRESSURE

REZA AKBARI ALASHTI, SEYED A. AHMADI

*Babol University of Technology, Department of Mechanical Engineering, Babol, Iran  
e-mail: raalashiti@nit.ac.ir*

In this paper, the effects of initial imperfections on the buckling behavior of thick cylindrical shells and curved panels are investigated. It is assumed that the shell has an axisymmetric and periodic initial imperfection in the axial direction. The shell is assumed to have different boundary conditions and subjected to pure external pressure loading. Governing differential equations are developed on the basis of the second Piola-Kirchhoff stress tensor and are reduced to a homogenous linear system of equations using the differential quadrature method. The effects of different boundary conditions, geometric ratios, curvature and imperfection parameter on the buckling behavior of isotropic thick cylindrical shells and curved panels are carefully discussed. The results obtained by the present method are verified with finite element solutions and those reported in the literature.

*Key words:* initial imperfection, buckling load, thick cylindrical panel

### 1. Introduction

Thick shells are widely used in various engineering applications, such as cooling towers, arch dams, oil and gas industries, pressure vessels, offshore and onshore structures. Since, these structures are often subjected to severe loading conditions, it is important to investigate their ultimate load carrying capacities. One of the most important failure modes of these structures is the loss of stability. Hence, it is vital to investigate their buckling behavior in various loading conditions. Several researches have been carried out on the buckling analysis of shells. Kardomateas (1993) studied the effect of thickness on the buckling load of a transversely isotropic thick cylindrical shell under axial compression. In his work, extensive study has been made on the performance of theories developed by Donnell (1933), Sanders (1963), Flugge (1960) and Danielson and Simmonds (1969) for the critical load prediction of a cylindrical shell made of an isotropic material and under the axial compression loading condition. Kardomateas (1996) also carried out three-dimensional buckling analysis of thick orthotropic cylindrical shells under combined loadings. The analytical solution based on the Donnell stability equation in the uncoupled form was reported by Brush and Almorth (1975). Bushnell (1985) carried out analytical and numerical calculations and experimental investigations on the buckling of shells. It was reported that analytical and experimental results were widely deviating. It was also reported that the cause for such deviation are the inevitable differences called imperfections which are present in the real structure and ignored in the perfect structural modeling. To achieve high structural performance of important structures such as offshore, aircraft and aerospace structures, it will be necessary to accurately predict critical conditions such as buckling phenomena of these structures. Ideally, highly accurate predictions of the buckling behavior of shells and curved panels can be obtained by appropriate consideration of their initial geometric imperfections, material properties, boundary conditions and other features. In most of these structures, imperfections are expected to be present, which are mainly produced during manufacturing process or caused by corrosion

pitting. Buckling analysis of thin shells with geometrical imperfection had been studied by few researchers. The effect of axisymmetric imperfections with axisymmetric buckling mode shapes on the stability behavior of isotropic and composite cylindrical shells under axial compression were investigated by Koiter (1980) and Elishakoff *et al.* (2001). Gusic *et al.* (2000) studied the effects of thickness variation in the circumferential direction and geometrical imperfections on the buckling behavior of thin cylindrical shells under the action of lateral pressure. Nguyen *et al.* (2009) investigated buckling behavior of cylindrical shells with variable thickness in the axial direction under the action of external pressure. Koiter (1963) presented an analytical formula for the buckling load of a perfect, non-uniform cylindrical shell under axial compression loading. Koiter *et al.* (1994) studied the influence of thickness variation on the buckling behavior of a cylindrical shell subjected to axial compression. They assumed the thickness variation to be axisymmetrical and very small compared with the shell thickness and showed that buckling load reduction is a linear function of the imperfection parameter when it is small.

In this work, three dimensional stability equations of shells and curved panels are developed on the basis of the second Piola-Kirchhoff stress tensor. The shell and panel are assumed to have different boundary conditions at the edges and be subjected to a pure lateral pressure loading. Also the influence of an axisymmetric and periodical imperfection on the buckling load of an isotropic thick cylindrical shell and a curved panel is investigated. The differential quadrature method is used to discrete differential equations and to obtain the buckling load of the thick cylindrical panel. Numerical results are compared with finite element solutions and results reported in the literature. Effects of various parameters including the boundary condition, panel curvature, imperfection amplitude factor and geometric ratios on the buckling behavior of the shell and curved panel are investigated.

## 2. Formulation of the problem

A thick cylindrical panel with the inner radius  $R_1$ , length  $L$ , curvature angle  $\beta$ , variable mid-surface radius  $a(x)$  and variable thickness  $h(x)$  is considered. The imperfection of the panel wall is assumed to be axisymmetric and periodic in the axial direction. The geometry, the coordinate system  $(r, \theta, x)$ , corresponding displacement components  $(w, v, u)$  and imperfection of the cylindrical panel are shown in Fig. 1. It is also assumed that the thicknesses of the shell obey the following formula

$$h(x) = h_0 \left[ 1 - \varepsilon \cos \frac{\pi}{L} \left( x - \frac{L}{2} \right) \right] \quad (2.1)$$

where  $h_0$  is the thickness of a perfect cylindrical panel and  $\varepsilon$  is the non-dimensional parameter of imperfection. According to the presented formulation, the mid-surface radius  $a(x)$  varies in the axial direction while the inner radius  $R_1$  is assumed to be constant. Also the thicknesses of the panel at two ends are the same for all values of  $\varepsilon$ , i.e.  $h(x) = h_0$  at  $x = 0, L$  and  $h(x) = h_0(1 - \varepsilon)$  at  $x = L/2$ . The value of  $\beta = 2\pi$  corresponds to the thick cylindrical shell.

The corresponding displacement functions at the perturbed position for the buckling state are expressed as

$$\begin{aligned} w(r, \theta, x) &= w^0(r, \theta, x) + \alpha w'(r, \theta, x) & v(r, \theta, x) &= v^0(r, \theta, x) + \alpha v'(r, \theta, x) \\ u(r, \theta, x) &= u^0(r, \theta, x) + \alpha u'(r, \theta, x) \end{aligned} \quad (2.2)$$

where  $\alpha$  is an infinitesimally small quantity;  $w^0(r, \theta, x)$ ,  $v^0(r, \theta, x)$  and  $u^0(r, \theta, x)$  denote initial values of components of the displacement field and  $w'(r, \theta, x)$ ,  $v'(r, \theta, x)$  and  $u'(r, \theta, x)$  denote values of the components of the displacement field in the disturbed position in the radial, circumferential and axial directions, respectively. The stress-strain relations for an isotropic material are defined as

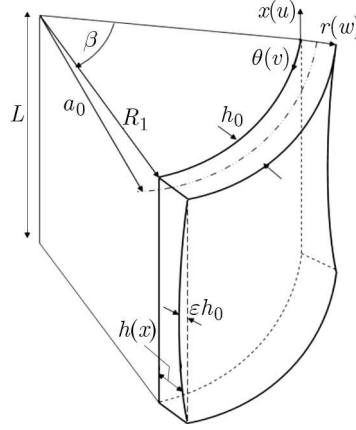


Fig. 1. Scheme of a curved panel, geometry, coordinates and axisymmetric imperfection

$$\begin{aligned}
 \sigma_{rr} &= (2G + \lambda)\varepsilon_{rr} + \lambda(\varepsilon_{\theta\theta} + \varepsilon_{xx}) & \tau_{r\theta} &= G\varepsilon_{r\theta} \\
 \sigma_{\theta\theta} &= (2G + \lambda)\varepsilon_{\theta\theta} + \lambda(\varepsilon_{xx} + \varepsilon_{rr}) & \tau_{rx} &= G\varepsilon_{rx} \\
 \sigma_{xx} &= (2G + \lambda)\varepsilon_{xx} + \lambda(\varepsilon_{\theta\theta} + \varepsilon_{rr}) & \tau_{x\theta} &= G\varepsilon_{x\theta}
 \end{aligned} \tag{2.3}$$

where  $\lambda$  and  $G$  are the Lamé coefficients

$$G(z) = \frac{E(z)}{2(1 + \nu)} \quad \lambda(z) = \frac{E(z)\nu}{(1 + \nu)(1 - 2\nu)} \tag{2.4}$$

By substituting the parameters of Eq. (2.2) into linear strain-displacement equations and using Eq. (2.3), strain and stress components in the perturbed configuration can be obtained in terms of the components of the displacement field.

The equations of equilibrium are written in terms of the second Piola-Kirchhoff stress tensor  $\boldsymbol{\sigma}$ , in following form (Lai, 1996)

$$\text{div}(\boldsymbol{\sigma} \cdot \mathbf{F}^T) = 0 \quad \mathbf{F} = \mathbf{I} + r \text{grad } \mathbf{V} \tag{2.5}$$

where  $\mathbf{F}$  is the deformation gradient,  $\mathbf{V}$  is the displacement vector and  $\mathbf{I}$  is the unit tensor. For a three dimensional problem, Eq. (2.5) can be expanded in the radial, circumferential and axial directions. Considering the linear normal strains  $\varepsilon_{ij} = \varepsilon_{ij}^0 + \alpha\varepsilon'_{ij}$  and rotations  $\omega_{ij} = \omega_{ij}^0 + \alpha\omega'_{ij}$  as well as stresses and keeping the linear terms in  $\alpha$ , a set of equations for the perturbed state is developed. The shear strain, shear stress and rotation are assumed to be zero in the initial conditions; hence the corresponding terms are dropped from the equilibrium equations. Since, the non-zero normal strains are assumed to be much smaller than 1, i.e.  $(1 + e_{rr}^0 \approx 1, 1 + e_{\theta\theta}^0 \approx 1, 1 + e_{xx}^0 \approx 1)$ , a system of homogeneous differential equations is obtained, which is linear in the derivatives of  $w, v, u$  with respect to  $r, \theta$  and  $x$

$$\begin{aligned}
 & \frac{\partial}{\partial r}(\sigma_{rr}^0\varepsilon'_{rr} + \sigma'_{rr}) + \frac{1}{r}\frac{\partial}{\partial\theta}[\tau'_{r\theta} + \sigma_{\theta\theta}^0(\varepsilon'_{r\theta} + \omega'_{r\theta})] + \frac{\partial}{\partial x}[\tau'_{rx} + \sigma_{xx}^0(\varepsilon'_{rx} + \omega'_{rx})] \\
 & \quad + \frac{1}{r}(\sigma'_{rr} + \sigma_{rr}^0\varepsilon'_{rr} - \sigma'_{\theta\theta} - \sigma_{\theta\theta}^0\varepsilon'_{\theta\theta}) = 0 \\
 & \frac{\partial}{\partial r}[\tau'_{r\theta} + \sigma_{rr}^0(\varepsilon'_{r\theta} - \omega'_{r\theta})] + \frac{1}{r}\frac{\partial}{\partial\theta}(\sigma_{\theta\theta}^0\varepsilon'_{\theta\theta} + \sigma'_{\theta\theta}) + \frac{\partial}{\partial x}[\tau'_{\theta x} + \sigma_{xx}^0(\varepsilon'_{\theta x} - \omega'_{\theta x})] \\
 & \quad + \frac{1}{r}[\sigma_{rr}^0(\varepsilon'_{r\theta} - \omega'_{r\theta}) + 2\tau'_{r\theta} + \sigma_{\theta\theta}^0(\varepsilon'_{r\theta} + \omega'_{r\theta})] = 0 \\
 & \frac{\partial}{\partial r}[\tau'_{rx} + \sigma_{rr}^0(\varepsilon'_{rx} - \omega'_{rx})] + \frac{\partial}{\partial x}(\sigma'_{xx} + \sigma_{xx}^0\varepsilon'_{xx}) + \frac{1}{r}\frac{\partial}{\partial\theta}[\sigma_{\theta\theta}^0(\varepsilon'_{\theta x} + \omega'_{\theta x}) + \tau'_{\theta x}] \\
 & \quad + \frac{1}{r}[\tau'_{rx} + \sigma_{rr}^0(\varepsilon'_{rx} - \omega'_{rx})] = 0
 \end{aligned} \tag{2.6}$$

### 3. Boundary condition

The boundary conditions of the shell are defined with the help of equilibrium equations using the second Piola-Kirchhoff tensor  $\boldsymbol{\sigma}$  as

$$(\mathbf{F} \cdot \boldsymbol{\sigma}) \cdot \mathbf{n} = \mathbf{t} \quad (3.1)$$

where  $\mathbf{t}$  is the traction vector and  $\mathbf{n}$  is the outward pointing unit normal vector. Applying the boundary conditions as defined in Eq. (3.1) for the initial and perturbed equilibrium positions, we have

$$\begin{aligned} \sigma'_{rr}\left(a + \frac{h}{2}, \theta\right) = \sigma'_{rr}\left(a - \frac{h}{2}, \theta\right) = 0 & \quad \tau'_{r\theta}\left(a + \frac{h}{2}, \theta\right) = \tau'_{r\theta}\left(a - \frac{h}{2}, \theta\right) = 0 \\ \tau'_{rx}\left(a + \frac{h}{2}, \theta\right) = \tau'_{rx}\left(a - \frac{h}{2}, \theta\right) = 0 & \end{aligned} \quad (3.2)$$

The stress components  $\sigma_{rr}^0$  and  $\sigma_{\theta\theta}^0$  at the outer and inner lateral surfaces of the shell due to the action of the lateral pressure  $p$  are given by the well known expressions from the linear elasticity theory (Ciarlet, 1988)

$$\begin{aligned} \sigma_{\theta\theta}^0 &= -p \left[1 + \left(\frac{R_1}{r}\right)^2\right] \left[1 - \left(\frac{R_1}{R_2}\right)^2\right]^{-1} = f_{\theta\theta}p \\ \sigma_{rr}^0 &= -p \left[1 - \left(\frac{R_1}{r}\right)^2\right] \left[1 - \left(\frac{R_1}{R_2}\right)^2\right]^{-1} = f_{rr}p \end{aligned} \quad (3.3)$$

Different types of boundary conditions are considered for the panel edges: Simply Supported (S), Clamped (C) and Free (F). The following boundary conditions are defined:

— simply supported (S):

$$\begin{aligned} \text{at } x = 0, L & \quad w = v = \sigma'_{xx} = 0 \\ \text{at } \theta = 0, \beta & \quad w = u = \sigma'_{\theta\theta} = 0 \end{aligned} \quad (3.4)$$

— clamped (C):

$$\begin{aligned} \text{at } x = 0, L & \quad w = v = u = 0 \\ \text{at } \theta = 0, \beta & \quad w = v = u = 0 \end{aligned} \quad (3.5)$$

— free (F):

$$\begin{aligned} \text{at } x = 0, L & \quad \sigma'_{xx} = \sigma'_{xr} = \sigma'_{x\theta} = 0 \\ \text{at } \theta = 0, \beta & \quad \sigma'_{\theta\theta} = \sigma'_{r\theta} = \sigma'_{x\theta} = 0 \end{aligned} \quad (3.6)$$

### 4. Buckling load calculation

Equations which are developed in the previous section include rotation and strain terms and can be used for general shells. Considering the linear strain-displacement equations and applying the stress-strain relations, i.e. Eq. (2.3), components of the stress field are defined in terms of components of the displacement field. Finally, by substituting the resulted expression in Eq. (2.6), the equilibrium equations in the buckled state are defined in terms of the components of the displacement field.

In the present study, a semi-analytical method called the differential quadrature method is used to discretize and solve the governing buckling equations. This method suggests that the

first order derivative of the function  $f(x)$  can be approximated as a linear sum of all functional values in the domain

$$\left. \frac{df}{dx} \right|_{x=x_i} = \sum_{j=1}^N w_{ij}^{(1)} f(x_j) \quad \text{for } i = 1, 2, \dots, N \quad (4.1)$$

where  $w_{ij}^{(1)}$  is the weighting coefficient and  $N$  denotes the number of grid points in the domain.

It should be noted that the weighting coefficients are different for different grid points of  $x_i$ . The polynomial and Fourier expansion methods are commonly used to determine the weighting coefficients. In this study, two types of differential quadratures are employed to approximate the first and second order derivatives of the function, namely the polynomial expansion based differential quadrature for the radial and the longitudinal directions and the Fourier expansion based differential quadratures for the circumferential direction (Shu, 2000).

Now, using the unequal spacing scheme for sampling points in the domain and applying the differential quadrature method for governing equations, we have

$$\begin{aligned} & (2G + \lambda) \sum_{l=1}^N a_{i,l}^{(2)} B_{l,j,k} + \frac{2G + \lambda}{r} \sum_{l=1}^N a_{i,l}^{(1)} B_{l,j,k} + G \sum_{n=1}^Q b_{j,n}^{(2)} B_{i,n,k} \\ & + (G + \lambda) \sum_{l=1}^N \sum_{n=1}^Q a_{i,l}^{(1)} b_{j,n}^{(1)} C_{l,n,k} - \frac{2G + \lambda}{r^2} B_{i,j,k} + \frac{G + \lambda}{r} \sum_{l=1}^N \sum_{m=1}^M a_{i,l}^{(1)} c_{k,m}^{(1)} A_{l,j,m} \\ & + \frac{G}{r^2} \sum_{m=1}^M c_{k,m}^{(2)} B_{i,j,m} + \frac{3G + \lambda}{r^2} \sum_{m=1}^M c_{k,m}^{(1)} A_{i,j,m} + \sigma_x^0 \sum_{n=1}^Q b_{j,n}^{(2)} B_{i,n,k} \\ & + P \left[ \frac{df_{rr}}{dr} \sum_{l=1}^N a_{i,l}^{(1)} B_{l,j,k} + f_{rr} \sum_{l=1}^N a_{i,l}^{(2)} B_{l,j,k} + \frac{f_{rr}}{r} \sum_{l=1}^N a_{i,l}^{(1)} B_{l,j,k} \right. \\ & \left. - \frac{f_{\theta\theta}}{r^2} \left( B_{i,j,k} - \sum_{m=1}^M c_{k,m}^{(2)} B_{i,j,m} - 2 \sum_{m=1}^M c_{k,m}^{(1)} A_{i,j,m} \right) \right] = 0 \\ & G \sum_{l=1}^N a_{i,l}^{(2)} A_{l,j,k} + \frac{G + \lambda}{r} \sum_{l=1}^N \sum_{m=1}^M c_{k,m}^{(1)} a_{i,l}^{(1)} B_{l,j,m} + \frac{3G + \lambda}{r^2} \sum_{m=1}^M c_{k,m}^{(1)} B_{i,j,m} + G \sum_{n=1}^Q b_{j,n}^{(2)} A_{i,n,k} \\ & + \frac{G}{r} \sum_{l=1}^N a_{i,l}^{(1)} A_{l,j,k} - \frac{G}{r^2} A_{i,j,k} + \frac{2G + \lambda}{r^2} \sum_{m=1}^M c_{k,m}^{(2)} A_{i,j,m} + \frac{G + \lambda}{r} \sum_{n=1}^Q \sum_{m=1}^M c_{k,m}^{(1)} b_{j,n}^{(1)} C_{i,n,m} \\ & + \sigma_x^0 \sum_{n=1}^Q b_{j,n}^{(2)} A_{i,n,k} + P \left[ \frac{df_{rr}}{dr} \sum_{l=1}^N a_{i,l}^{(1)} A_{l,j,k} + f_{rr} \sum_{l=1}^N a_{i,l}^{(2)} A_{l,j,k} \right. \\ & \left. + \frac{f_{rr}}{r} \sum_{l=1}^N a_{i,l}^{(1)} A_{l,j,k} - \frac{f_{\theta\theta}}{r^2} \left( A_{i,j,k} - \sum_{m=1}^M c_{k,m}^{(2)} A_{i,j,m} - 2 \sum_{m=1}^M c_{k,m}^{(1)} B_{i,j,m} \right) \right] = 0 \\ & G \sum_{l=1}^N a_{i,l}^{(2)} C_{l,j,k} + (2G + \lambda) \sum_{n=1}^Q b_{j,n}^{(2)} A_{i,n,k} + (G + \lambda) \sum_{l=1}^N \sum_{n=1}^Q b_{j,n}^{(1)} a_{i,l}^{(1)} B_{l,n,k} + \frac{G}{r} \sum_{l=1}^N a_{i,l}^{(1)} C_{l,j,k} \\ & + \frac{G}{r^2} \sum_{m=1}^M c_{k,m}^{(2)} C_{i,j,m} + \frac{G + \lambda}{r} \sum_{m=1}^M c_{k,m}^{(1)} A_{i,j,m} + \frac{G + \lambda}{r} \sum_{n=1}^Q b_{j,n}^{(1)} B_{i,n,k} + \sigma_x^0 \sum_{n=1}^Q b_{j,n}^{(2)} C_{i,n,k} \\ & + P \left[ \left( \frac{df_{rr}}{dr} + \frac{f_{rr}}{r} \right) \sum_{l=1}^N a_{i,l}^{(1)} C_{l,j,k} + 2f_{rr} \sum_{l=1}^N a_{i,l}^{(2)} C_{l,j,k} + \frac{f_{\theta\theta}}{r^2} \sum_{m=1}^M c_{k,m}^{(2)} C_{i,j,m} \right] = 0 \end{aligned} \quad (4.2)$$

where  $a_{ij}^{(k)}$ ,  $b_{ij}^{(k)}$  and  $c_{ij}^{(k)}$  denote weighting coefficients of the  $k$ -th order derivative in the  $r$ ,  $\theta$  and  $x$ -direction, respectively;  $N$ ,  $Q$  and  $M$  are grid point numbers in the  $r$ ,  $\theta$  and  $x$ -direction,

respectively. Also, it must be noted that the boundary conditions have been discretized by the differential quadrature method. The critical value of the external pressure  $P_{cr}$ , i.e. the buckling load, is calculated by solving the set of equations which are transformed into the standard eigenvalue equation of the following form

$$\left(-[\mathbf{DBG}][\mathbf{BB}]^{-1}[\mathbf{BD}]+[\mathbf{DDG}]\right)^{-1}\left(-[\mathbf{DB}][\mathbf{BB}]^{-1}[\mathbf{BD}]+[\mathbf{DD}]\right)[u, v, w]^T - P\mathbf{I}[u, v, w]^T = \mathbf{0} \quad (4.3)$$

where the sub-matrices  $[\mathbf{BB}]$ ,  $[\mathbf{BD}]$  and  $[\mathbf{DBG}]$ ,  $[\mathbf{DD}]$ ,  $[\mathbf{DB}]$ ,  $[\mathbf{DDG}]$  result from the boundary conditions and governing equations, respectively.

## 5. Numerical results and discussion

In this section, accuracy of the present method is validated against the results reported in the literature. The normalized results of stability equations for an isotropic thick cylindrical shell under the action of pure axial compression obtained by the differential quadrature method are presented in Table 1. For this specific case, Young's modulus  $E$  of the shell is considered to be 14 GPa. In this work, for complete cylindrical shells, the perturbed displacements are assumed to be in the following form

$$\begin{aligned} w(r, \theta, x) &= B(r, x) \cos(m\theta) & v(r, \theta, x) &= A(r, x) \sin(m\theta) \\ u(r, \theta, x) &= C(r, x) \cos(m\theta) \end{aligned} \quad (5.1)$$

where  $m$  is the buckling mode in the circumferential direction. Considering relations (5.1), we obtain a new set of equations that are simpler than equations (4.2). It is observed from this table that the results are in good agreement with the reported results for thick shells.

**Table 1.** Normalized buckling load of the shell under pure axial compression  $E = 14 \text{ GN/m}^2$ ,  $h = R_2 - R_1$ ,  $\nu = 0.3$ ,  $R_2 = 1 \text{ m}$ ,  $L/R_2 = 5 \text{ m}$ , critical load:  $f = FR_2/\pi Eh(R_2^2 - R_1^2)$

$R_2/R_1$	Present paper	Kardomateas (1996)	Flügge (1960)
1.15	0.4278 (2)	0.4547 (2,1)*	0.4710 (2,1)
1.2	0.4176 (2)	0.4371 (2,2)	0.4620 (2,2)
1.25	0.4191 (2)	0.4426 (2,2)	0.4728 (2,2)
1.3	0.4749 (1)	0.4487 (1,1)	0.4915 (1,1)

\*  $(m, n)$  denote buckling mode numbers in the circumferential and axial directions, respectively

To study the buckling behavior of a shell with an imperfection, a quantity,  $\lambda$  denoting the ratios of the buckling loads of the imperfect shell to the perfect shell is considered

$$\lambda = \frac{P_{cr}^{(imper)}}{P_{cr}^{(per)}} \quad (5.2)$$

In this work, it is assumed that the shell is made of aluminum with the elastic modulus  $E = 70 \text{ GPa}$  and Poisson's ratio of 0.3. The critical buckling modes of the shell are taken as  $m_{cr} = 2.7\sqrt{a_0/L}\sqrt[4]{a_0/h_0}$ . The shell is assumed to have clamped boundary conditions at two ends. The results of stability equations obtained by the present method for different values of the imperfection parameter  $\varepsilon$  for a thick shell with  $R_2/R_1 = 1.2$  and  $L/a_0 = 1$  are compared with the finite element results as shown in Table 2. Comparison of the results presented in

Table 2, indicates a very good agreement between these results for lower values of the imperfection parameter  $\varepsilon$ . Variation of the buckling load reduction parameter  $\lambda$  of a thick shell with imperfection subjected to pure external pressure loading is presented in Fig. 2. It is found that the buckling load reduction parameter has linear variation with the ratio of the outer-to-inner radius of the shell  $R_2/R_1$  for higher values of  $\varepsilon$ . It is also noted that geometrical imperfections have higher effects on the buckling load of thick shells than thin shells. On the other hand, the rate of buckling load reduction with  $\varepsilon$  increases for thicker shells. These results propose the same pattern as presented by Nguyen *et al.* (2009) for simply supported thin shells.

**Table 2.** Normalized buckling pressure and buckling load reduction for pure lateral loading of an imperfect shell

$\varepsilon$	Present		FEM	
	$P_{cr}R_2/Eh$	$\lambda$	$P_{cr}R_2/Eh$	$\lambda$
0	0.1266	1	0.1254	1
0.01	0.1240	0.979	0.1222	0.974
0.05	0.1155	0.912	0.1138	0.906
0.10	0.1028	0.811	0.1022	0.814
0.15	0.0897	0.708	0.0882	0.712
0.20	0.0768	0.607	0.0762	0.615

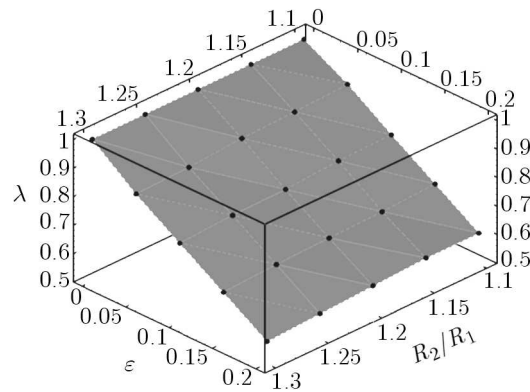


Fig. 2. Variation of the buckling load reduction factor  $\lambda$  with  $\varepsilon$  and the ratio of  $R_2/R_1$

Variation of critical pressures with the mode number of a thick cylindrical shell with imperfection is presented in Fig. 3. It is revealed from this figure that the critical loads for higher values of  $m$  approaches an asymptotic value, and the buckling load ratio  $\lambda$  remains constant.

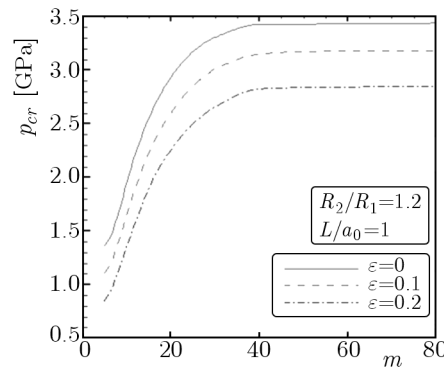


Fig. 3. Variation of the critical pressure versus  $m$  for a thick cylindrical shell

The effect of the ratio of the length-to-mid-plane radius, i.e.  $L/a_0$  on the critical load of an imperfect cylindrical shell with  $R_2/R_1 = 1.2$  subjected to uniform lateral pressure is shown in Fig. 4. The results are given for the buckling mode number  $m = 2$ . It is realized from Fig. 4 that as the ratio of  $L/a_0$  increases, the buckling load approaches an asymptotic value.

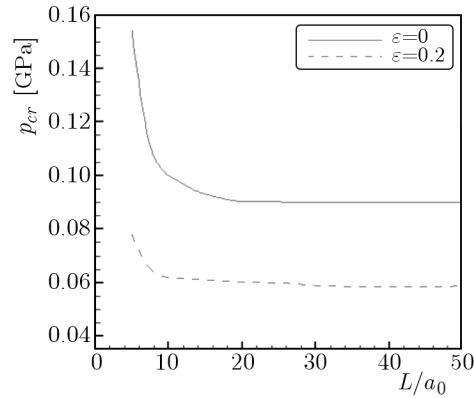


Fig. 4. Variation of the buckling pressure of a thick imperfect shell versus  $L/a_0$

Next, the effect of the imperfection parameter  $\varepsilon$  on the buckling behavior of a thick cylindrical shell under the action of uniform external pressure is investigated. Buckling loads for various ratios of the external-to-internal radius of the shell with  $L/a_0 = 1$  are shown in Fig. 5. It is evident from the figure that for small values of  $\varepsilon$ , the imperfection has a higher effect on the buckling behavior of the shell under lateral pressure loading, however the rate of reduction of the buckling load reduces as the load factor increases. It is also found that as the thickness of the shell increases, the variation of the buckling pressure increases with the imperfection parameter.

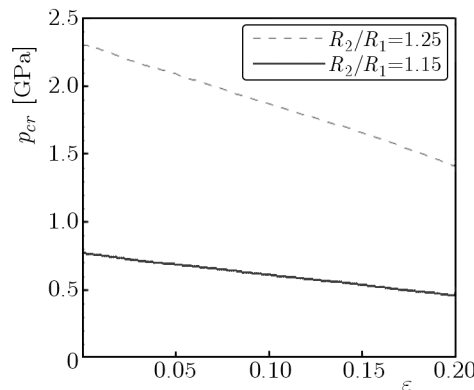


Fig. 5. Variation of the critical pressure with  $\varepsilon$

In this part, in order to study the effect of boundary conditions on the buckling behavior of thick cylindrical shells, the results for different ratios of  $R_2/R_1$  are shown in Fig. 6. Different boundary conditions such as simply supported (S), clamped (C) and free (F) are considered for the shell. It can be seen that, as expected, the shell with clamped-clamped boundary condition has a higher buckling load than other shells, and the one with free boundary conditions has a very low buckling pressure.

Buckling pressures and the buckling load reduction parameter  $\lambda$  for an imperfect thick shell under the action of pure external pressure loading with various boundary conditions are presented in Table 3. As shown in the table, in the case of the simply supported condition, the imperfections have a higher effect on the buckling behavior of shells, and the rate of decrease of the buckling load reduction parameter is higher than for other boundary conditions.

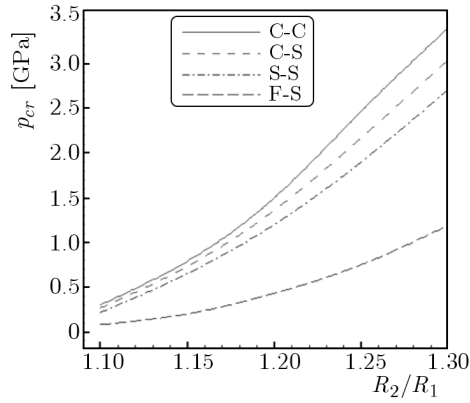


Fig. 6. Effect of the boundary condition on the buckling pressure of a cylindrical shell

**Table 3.** The buckling pressure and buckling load reduction parameter for different boundary conditions

$\varepsilon$	C-C		S-C		S-S	
	$p_{cr}$ [GPa]	$\lambda$	$p_{cr}$ [GPa]	$\lambda$	$p_{cr}$ [GPa]	$\lambda$
1	1.52	1	1.38	1	1.2	1
0.01	1.497	0.978	1.356	0.983	1.177	0.981
0.05	1.36	0.9	1.23	0.89	1.061	0.884
0.1	1.205	0.793	1.08	0.783	0.919	0.766
0.15	1.056	0.695	0.93	0.674	0.783	0.653
0.18	0.97	0.638	0.85	0.616	0.703	0.586
0.2	0.912	0.6	0.79	0.572	0.65	0.54

Next, the buckling behavior of a thick cylindrical panel with different boundary conditions is investigated. Various boundary conditions are considered for edges of the panel as shown in Fig. 7. The variation of buckling pressure for two sets of boundary conditions versus the panel angle  $\beta$  is presented in Fig. 8. It is assumed that the geometrical parameters of the shell are  $L/a_0 = 1$  and  $R_2/R_1 = 1.2$ . It can be seen that the buckling load decreases and approaches an asymptotic value as  $\beta$  increases.

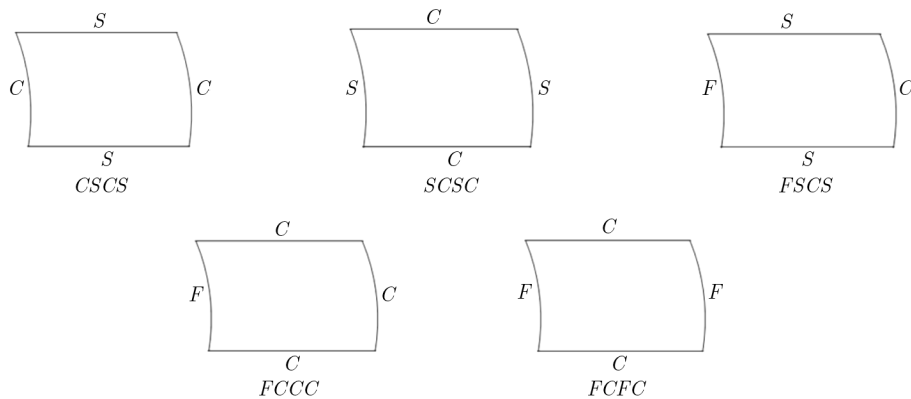


Fig. 7. Boundary conditions for a thick panel

Buckling pressures in GPa for different ratios of the external-to-internal radius  $R_2/R_1$  for thick panels with  $L/a_0 = 1$  and  $\beta = \pi/2$  are given in Table 4. Different boundary conditions are considered for edges as shown in Fig. 7. It is revealed from this figure that the panel with

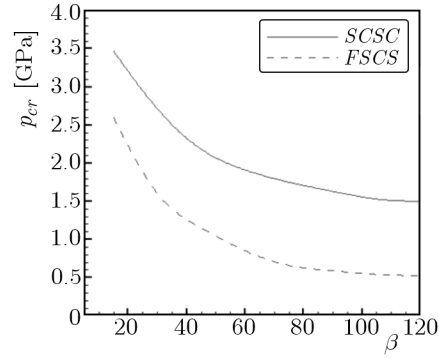


Fig. 8. Effect of panel curvature on the buckling pressure of a thick panel

the CSCS boundary condition has the largest buckling load. For the case of  $R_2/R_1 = 1.2$  and various boundary conditions according to Table 4, the buckling modes obtained by finite element software ANSYS are shown in Fig. 9.

**Table 4.** Buckling pressure of the panel with  $\beta = \pi/2$  versus  $R_2/R_1$  for various boundary conditions

$R_2/R_1$	CSCS	SCSC	FCCC	FCFC	FSCS
1.05	0.066	0.0597	0.051	0.042	0.026
1.1	0.392	0.33	0.3	0.24	0.12
1.15	0.984	0.87	0.67	0.59	0.31
1.2	1.74	1.6	1.25	1.16	0.604
1.25	2.58	2.43	1.94	1.8	0.98
1.3	3.44	3.3	2.66	2.4	1.8

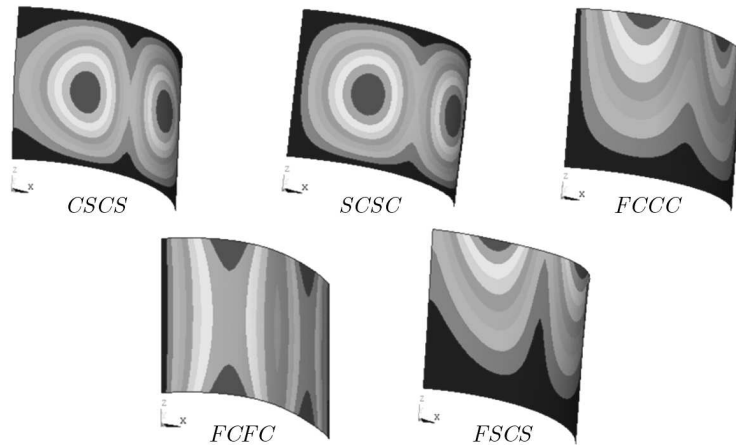


Fig. 9. Buckling modes of panels,  $\beta = \pi/2$ , with different boundary conditions

The effects of geometrical imperfections on the ultimate load carrying capacity of panels are studied. The buckling pressures and buckling load reductions for panels with  $L/a_0 = 1$ ,  $R_2/R_1 = 1.2$  and different boundary conditions are presented in Table 5. Among given boundary conditions in Table 5, the buckling response of panels with four clamped edges is more sensitive to the imperfection parameter than in other cases.

**Table 5.** The buckling pressure and buckling load reduction of the panel,  $\beta = \pi/2$ , for different boundary conditions

$\varepsilon$	CCCC		FCCC		CSCS		FSCS	
	$p_{cr}$ [GPa]	$\lambda$						
0	1.74	1	1.25	1	1.53	1	0.604	1
0.05	1.59	0.91	1.19	0.952	1.39	0.91	0.597	0.98
0.10	1.435	0.82	1.117	0.894	1.25	0.82	0.58	0.95
0.15	1.29	0.74	1.03	0.826	1.11	0.73	0.54	0.90
0.20	1.14	0.65	0.94	0.75	0.98	0.64	0.512	0.84

## 6. Conclusion

In the present paper, the stability equations of thick cylindrical panels are obtained using the benchmark three-dimensional elasticity solution. The buckling analysis of such panels under the action of uniform lateral pressure loading is carried out. Different boundary conditions, namely simply supported, clamped and free are considered for the edges of panels. The effect of an axisymmetric and periodic initial imperfection on the critical buckling load of the panel is investigated. The resulting differential equations are discretized and solved by the differential quadrature method. Effects of the shell geometric and imperfection parameters and boundary conditions on the buckling behavior of cylindrical shells and panels are investigated. It is found that the initial imperfection can significantly reduce ultimate load carrying capacities of these structures. Such a limit load reduction is found to be linear for small values of the thickness imperfection parameter  $\varepsilon$ . It is also shown that the imperfections have higher effects on the buckling behavior of thick panels than on thin ones.

## References

- BRUSH D.O., ALMROTH B.O., 1975, *Buckling of Bars, Plates and Shells*, Chapter 5, McGraw-Hill, New York
- BUSHNELL D., 1985, *Computerized Buckling Analysis of Shells*, Martinus Nijhoff Publishers, Dordrecht
- CIARLET P.G., 1988, *Mathematical Elasticity, Vol. I, Three Dimensional Elasticity*, North-Holland: Amsterdam
- DANIELSON D.A., SIMMONDS, J.G., 1969, Accurate buckling equations for arbitrary and cylindrical elastic shells, *International Journal of Engineering Science*, **7**, 459
- DONNELL L.H., 1933, *Stability of Thin-Walled Tubes Under Torsion*, NACA Rep. 479
- ELISHAKOFF I., LI Y., STARNERS J.H., 2001, *Non-Classical Problem in Theory of Elastic Stability*, Cambridge University Press, Cambridge, 43-98
- FLUGGE W., 1960, *Stresses in Shells*, Springer-Verlag, Berlin, Heidelberg
- GUSIC G., COMBESURE A., JULLIEN J.F., 2000, The influence of circumferential thickness variations on the buckling of cylindrical shells under lateral pressure, *Computer Structures*, **74**, 461-477
- KARDOMATEAS G.A., 1993, Stability loss in thick transversely isotropic cylindrical shells under axial compression, *Journal of Applied Mechanics (ASME)*, **60**, 506
- KARDOMATEAS G.A., 1996, Benchmark three-dimensional elasticity solution for the buckling of thick orthotropic cylindrical shells, *Composites, Part B*, **27**, B(6), 569-580
- KOITER W.T., 1963, The effect of axisymmetric imperfection on the buckling of cylindrical shells under axial compression, *Academia van Wetenschappen-Amsterdam, Series B*, **66**, 265-279

12. KOITER W.T., 1980, Buckling of cylindrical shells under axial compression and external pressure: Thin shell theory new trends and applications, [In:] *CISM Courses and Lectures*, **40**, W. Olszak (Edit.), Wien and New York, Springer, 77-87
13. KOITER W.T., ELISHAKOFF I., LI Y.W., STARNES J.H., 1994, Buckling of an axially compressed cylindrical shell of variable thickness, *International Journal of Solids and Structures*, **31**, 6, 797-805
14. LAI W.M., RUBIN D., KREML E., 1996, *Introduction to Continuum Mechanics*, 3rd ed. Butterworth-Heinemann, Massachusetts
15. NGUYEN T.H.L., ELISHAKOFF I., NGUYEN T.V., 2009, Buckling under external pressure of cylindrical shell with variable thickness, *International Journal of Solids and Structures*, **46**, 4163-68
16. SANDERS J.L., 1963, Nonlinear theories of thin shells, *Quarterly of Applied Mathematics*, **21**
17. SHU C., 2000, *Differential Quadrature and its Application in Engineering*, London, Springer-Verlag

*Manuscript received February 21, 2013; accepted for print May 12, 2013*